



High-resolution map of the Fc functions mediated by COVID-19-neutralizing antibodies

Ida Paciello^a, Giuseppe Maccari^b, Elisa Pantano^a, Emanuele Andreano^{a,1}, and Rino Rappuoli^{c,d,1}

Contributed by Rino Rappuoli; received September 4, 2023; accepted December 1, 2023; reviewed by Barney S. Graham and Hedda Wardemann

A growing body of evidence shows that fragment crystallizable (Fc)-dependent antibody effector functions play an important role in protection from severe acute respiratory syndrome coronavirus 2 (SARS-CoV-2) infection. To unravel the mechanisms that drive these responses, we analyzed the phagocytosis and complement deposition mediated by a panel of 482 human monoclonal antibodies (nAbs) neutralizing the original Wuhan virus, expressed as recombinant IgG1. Our study confirmed that nAbs no longer neutralizing SARS-CoV-2 Omicron variants can retain their Fc functions. Surprisingly, we found that nAbs with the most potent Fc function recognize the N-terminal domain, followed by those targeting class 3 epitopes in the receptor binding domain. Interestingly, nAbs direct against the class 1/2 epitopes in the receptor binding motif, which are the most potent in neutralizing the virus, were the weakest in Fc functions. The divergent properties of the neutralizing and Fc function–mediating antibodies were confirmed by the use of different B cell germlines and by the observation that Fc functions of polyclonal sera differ from the profile observed with nAbs, suggesting that non-neutralizing antibodies also contribute to Fc functions. These data provide a high-resolution picture of the Fc-antibody response to SARS-CoV-2 and suggest that the Fc contribution should be considered for the design of improved vaccines, the selection of therapeutic antibodies, and the evaluation of correlates of protection.

SARS-CoV-2 | antibodies | Fc function | B cell germlines

The coronavirus disease 2019 (COVID-19) pandemic has been responsible for more than 768 million infections and nearly 7 million deaths reported worldwide (1). Significant progress in the fight against severe acute respiratory syndrome coronavirus 2 (SARS-CoV-2) has been achieved with the approval and the administration of vaccines and monoclonal antibodies (mAbs). Antibodies administrated or elicited by vaccination neutralize viral entry into host cells by the interaction between the antigen-binding fragment (Fab) region of the antibodies and the SARS-CoV-2 Spike (S) protein (2, 3). Early predictive models suggested that neutralizing levels of anti-S protein antibodies elicited by vaccination correlate with protection from infection with SARS-CoV-2 (4). These studies were conducted when the S protein antigen encoded by COVID-19 vaccines was the same as the circulating virus. Unfortunately, during the COVID-19 pandemic, SARS-CoV-2 variants developed progressively several mutations mainly placed in the receptor binding domain (RBD) and the N-terminal domain (NTD) of the S protein (5). These SARS-CoV-2 variants, and especially the Omicron lineages, show resistance against the majority of monoclonal antibodies and the ability to evade infection and vaccination-induced immunity (6, 7). As a result, higher neutralizing antibody titers are necessary to induce protection from SARS-CoV-2 variants (8). Despite elevated resistance to neutralization, individuals infected with recently emerged variants showed lower severity of disease, suggesting that additional components of the immune system play a role in protection from severe COVID-19 (9). Fragment crystallizable (Fc)-dependent antibodies effector functions are emerging as key players in determining the outcome of severe infection (10, 11). Several pieces of evidence report that the Fc functions provide protection from COVID-19 diseases even in the absence of neutralization (10–12). Indeed, Addetia et al. demonstrated that the FDA-approved mAb S309 (sotrovimab) triggers antibody-dependent cell cytotoxicity (ADCC) *in vitro* and protects mice against BQ.1.1 challenge *in vivo* despite loss of neutralization activity (12). In addition, Mackin et al. reported that mice lacking expression of activating Fc γ Rs, especially murine Fc γ R III (CD16), or depleted of alveolar macrophages, lose the antiviral activity of passively transferred immune serum against multiple SARS-CoV-2 variants (10). Recent serology data have also demonstrated that SARS-CoV-2 vaccine induced higher Fc-receptor binding antibody levels and consequently higher humoral and cellular immune responses in subjects with previous SARS-CoV-2 infection compared to infection of naive individuals. In addition to SARS-CoV-2, several studies reported that Fc-effector functions are also crucial to confer

Significance

The COVID-19 pandemic highlighted the need to deeply understand which arms of the immune system are responsible for protection from severe infection. Antibody neutralization has been the main indicator of protection, but increasing evidence highlights the role of fragment crystallizable (Fc) effector functions in determining the outcome of severe acute respiratory syndrome coronavirus 2 infection. In this study, we investigated at the single cell level the Fc functions mediated by a panel of 482 neutralizing human monoclonal antibodies unravelling the S protein domains, the specific epitopes, and B cell germlines mainly involved in this response. In addition, we identified the key differences that drive the neutralization and Fc-mediated activities in infected and vaccinated donors highlighting the features that characterize these distinct cohorts.

Author contributions: I.P., E.A., and R.R. designed research; I.P. performed research; E.P. contributed new reagents/analytic tools; I.P., E.A., and G.M. analyzed data; and I.P., E.A., and R.R. wrote the paper.

Reviewers: B.S.G., Morehouse School of Medicine; and H.W., Deutsches Krebsforschungszentrum.

Competing interest statement: R.R. owns Novartis and GSK stocks. I.P., E.P., E.A., and R.R. are listed as inventors of full-length human monoclonal antibodies described in Italian patent applications no. 102020000015754 filed on June 30th 2020, 102020000018955 filed on August 3rd 2020 and 102020000029969 filed on 4th of December 2020, and the international patent system number PCT/IB2021/055755 filed on the 28th of June 2021. All patents were submitted by Fondazione Toscana Life Sciences, Siena, Italy. Remaining authors have no competing interests to declare.

Copyright © 2024 the Author(s). Published by PNAS. This open access article is distributed under Creative Commons Attribution-NonCommercial-NoDerivatives License 4.0 (CC BY-NC-ND).

¹To whom correspondence may be addressed. Email: e.andreano@toscanalifesciences.org or rino.rappuoli@biotecnopolito.it.

This article contains supporting information online at <https://www.pnas.org/lookup/suppl/doi:10.1073/pnas.2314730121/-DCSupplemental>.

Published January 10, 2024.

protection against other pathogens including influenza virus (13, 14), Ebola virus (15), and several bacterial infections (16). Given the relevance of the Fc-mediated functions, it becomes of utmost importance to understand which are the epitopes and B cell germlines involved in this response and if they overlap with those inducing neutralizing antibodies. To answer this question, we took advantage of our unique panel of 482 Wuhan neutralizing human monoclonal antibodies (nAbs), most of which lost their neutralization activity against Omicron variants (17). These antibodies derived from naive donors who were immunized with two mRNA vaccine doses (Seronegative, SN2) and subsequently re-enrolled after receiving the third vaccine dose (Seronegative, SN3), and convalescent donors who had been infected before vaccination (Seropositive, SP2) (18, 19). Antibody-dependent cellular phagocytosis (ADCP) and antibody-dependent complement-dependent deposition (ADCD) were used to characterize at a single-cell level the Fc-effector functions of our nAb panel. These functions depend on antibody isotype, location and geometry of the antibody-binding epitope, stoichiometry of the antibody to antigen, and affinity of the antibody for both its antigen and its cognate FcR (11). To investigate the influence of the SARS-CoV-2 S protein domains and epitopes to induce Fc activities, all nAbs were expressed as recombinant IgG1 isotypes. Our data revealed that nAbs that lost their neutralization activity can retain Fc functions against tested Omicron variants and shared key features among infected and vaccinated donors. In particular, different domains, epitopes, and B cell germlines were shown to drive Fc functions and the neutralization response. These data suggest that synergy between Fc-mediated functions and neutralization could be a successful strategy to design improved vaccines and therapeutics against COVID-19.

Results

Hybrid Immunity Induces High Fc-Dependent Effector Functions

Polyclonal Antibody Response. To explore the polyclonal response elicited by infection and vaccination, we collected plasma samples from seronegative subjects immunized with two (SN2, n = 5) or three (SN3, n = 4) mRNA vaccine doses (18, 19) and seropositive donors who had been infected before mRNA vaccination (SP2, n = 5). As a first step, we evaluated the ability of the polyclonal antibody response to drive cellular phagocytosis through an ADCP assay, evaluated by measuring the THP-1 engulfment of beads coated with fluorescent S proteins (Fig. 1A). The uptake of S protein-coated beads was confirmed by the morphological change observed in THP-1 when assessed by flow cytometry (*SI Appendix*, Fig. S1A and B). SP2 induced the highest ADCP activity to all SARS-CoV-2 S proteins, followed by SN3 and SN2 (Fig. 1B). The ADCP activity slightly decreased with BA.1 and had a dramatic reduction with BA.2. However, the ADCP activity of SP2 remained the highest (Fig. 1B). Next, we evaluated the ADCC response in SN2, SN3, and SP2. As illustrated in Fig. 1C, Expi293F cells expressing SARS-CoV-2 Wuhan, BA.1, or BA.2 S protein were incubated with plasma samples, and the C3 deposition was measured through flow cytometry (*SI Appendix*, Fig. S1C). In line with ADCP results, SP2 subjects showed the highest ADCC activity followed by SN3 and SN2 (Fig. 1D). The Omicron variants showed a drastic reduction in ADCC activity in all cohorts with almost complete evasion of this response in SN2 and SN3. In fact, BA.1 showed a 2.5-fold, 3.2-fold, and 4.1-fold ADCC reduction in SN2, SN3, and SP2, respectively. Similarly, the use of BA.2 S protein led to a 2.1-fold, 2.7-fold, and 3.3-fold ADCC decrease in SN2, SN3, and SP2, respectively (Fig. 1D).

ADCP Is Driven by NTD-Targeting nAbs after a Third mRNA Vaccine Dose and Hybrid Immunity. Next, we characterized the ADCP of neutralizing monoclonal antibodies (nAbs) isolated from SARS-CoV-2 naive donors after two (SN2; n = 52), three vaccinations (SN3, n = 206) and 224 nAbs derived from subjects vaccinated after COVID-19 infection (SP2) (18, 19). These nAbs were isolated from class-switched memory B cells (CD19⁺CD27⁺IgD⁻IgM⁺). Therefore, our total nAb panel is composed of 482 antibodies neutralizing the Wuhan virus of which 74 to 98% had lost the ability to neutralize Omicron BA.1 and BA.2 variants (17). To specifically assess and identify the S protein domains and epitopes involved in Fc functions, all nAbs were expressed as IgG1. Therefore, the Fc functions observed depend on the antibody-binding epitope site, the stoichiometry and affinity of the antibody Fab region for its antigen. Up to 99.4% (n = 479) of nAbs induced phagocytosis activity against the Wuhan SARS-CoV-2 S protein (Fig. 2A). However, the overall potency of ADCP in SN2 is significantly lower than that of SN3 and SP2 (SN2 vs. SN3 P < 0.0001; SN2 vs. SP2 P < 0.001) (Fig. 2A). Over 70% and 60% of nAbs in the SP2 and SN3 cohorts showed high ADCP activity, respectively, while only 35% of this class of antibodies was found in the SN2 group. For this screening, an unrelated plasma was used as negative control, and the threshold for sample positivity was set at threefold the ADCP score of the negative control. Based on this cutoff point, nAbs were classified as high (>eightfold the threshold), medium (>fourfold the threshold), or low (up to fourfold the threshold) phagocytosis inducers, and given the extent of our nAb panel, antibodies were tested at a single-point dilution. Then, we tested the ADCP against the Omicron BA.1 and BA.2 lineages. Overall, nAbs tested displayed a significantly lower ADCP activity against the Omicron variants compared to Wuhan (Fig. 2A). Only 15.5% (9/52) and 25.0% (56/224) of nAbs in the SN2 and SP2 cohorts, respectively, retained ADCP against BA.1. Conversely, up to 60.7% (125/206) of tested antibodies in the SN3 group drove phagocytosis although with much lower ADCP titers. A different scenario was observed against the Omicron BA.2, where only 25.7% (53/206) of nAbs derived from the SN3 cohort induced opsonization which was similar to what was observed in the SN2 group (7/52; 13.5%). An opposite trend was observed in the SP2 cohort, where 31.7% (71/224) of nAbs drove ADCP against the Omicron BA.2 which was significantly higher to that observed in the SN3 group. To confirm that ADCP titers obtained were independent from the antibody concentration, a nAb dose-phagocytosis titer correlation was performed. The analyses showed that the S protein-dependent opsonization levels were unrelated to the antibody concentration used (*SI Appendix*, Fig. S2A). Moreover, additional correlation analysis revealed that there was no correlation between neutralization and ADCP titers for all SARS-CoV-2 variants tested (*SI Appendix*, Fig. S2B–D). In our previous work, we identified the S protein domain recognized by our nAb panel. To better understand the impact of S protein domains, we analyzed the ADCP activity of the 369 RBD-binding antibodies (SN2 = 37, SN3 = 154, and SP2 = 178), the 89 NTD-targeting nAbs (SN2 = 9, SN3 = 43, and SP2 = 37) and the 24 antibodies that bind to the S protein trimer (SN2 = 6, SN3 = 9, and SP2 = 9) (17). Compared to RBD and NTD-targeting nAbs, the low numbers of S protein trimer-targeting nAbs are a limit of the analysis for this group of antibodies. We exploited this information to understand which domains were mainly responsible for ADCP. Our data showed that almost all nAbs, independently from the targeted domain, were able to induce phagocytosis against the Wuhan SARS-CoV-2 virus. However, both ADCP frequency (Fig. 2B–D, Left and *SI Appendix*, Table S1) and potency (Fig. 2B–D, Right and *SI Appendix*, Table S2) are

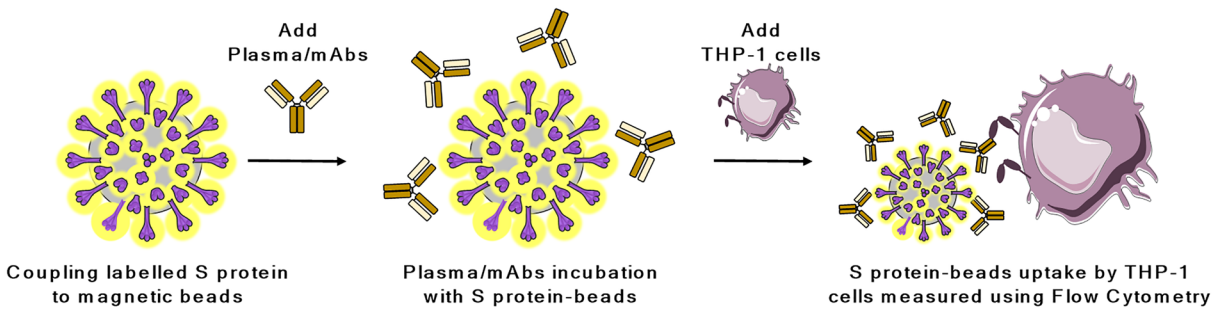
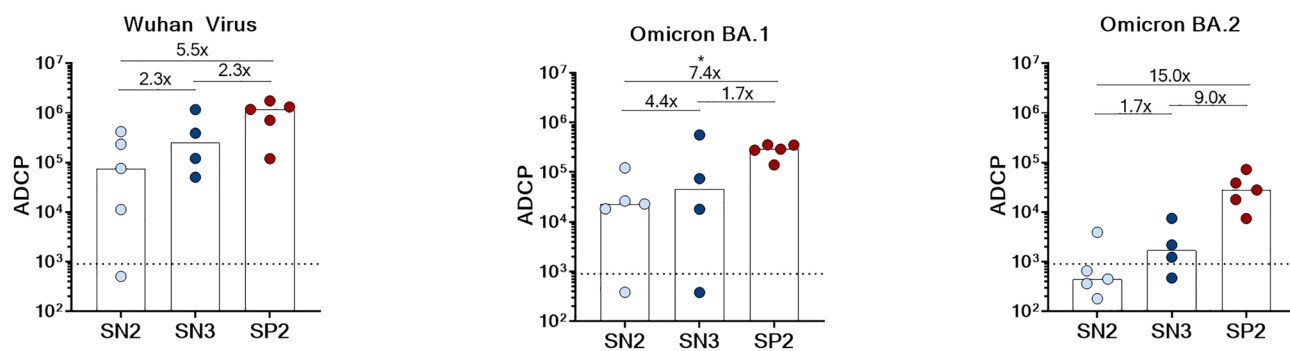
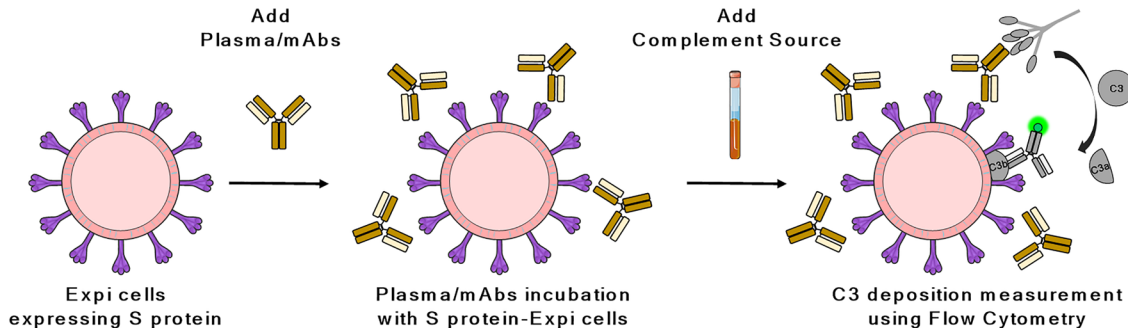
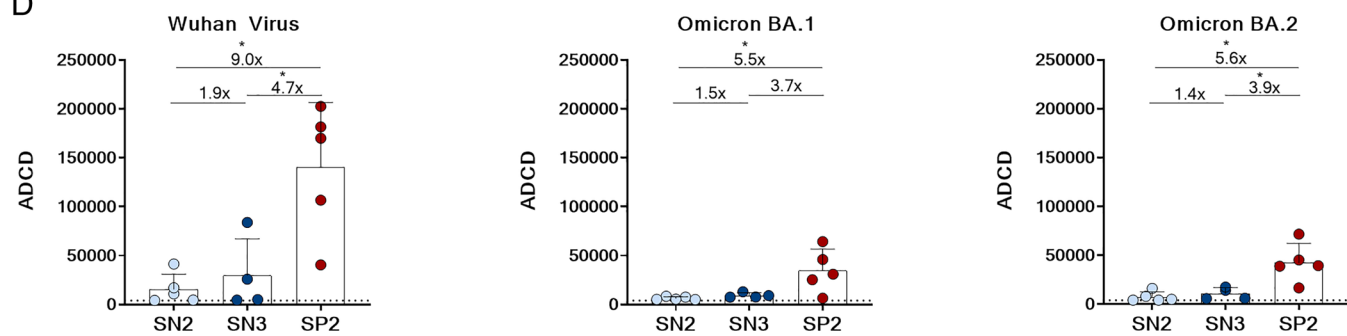
A**Antibody dependent Cellular Phagocytosis (ADCP)****B****C****Antibody dependent Complement Deposition (ADCD)****D**

Fig. 1. ADCP and ADCC driven by polyclonal response. (A) Schematic representation of the ADCP assay. (B) Comparison of ADCP activity against SARS-CoV-2 WT, BA.1, and BA.2 variants in THP-1 incubated with plasma derived from SN2, SN3, and SP2 cohorts. (C) Illustration of the ADCC assay performed. (D) Comparison of ADCC activity of plasma derived from SN2, SN3, and SP2 cohorts against SARS-CoV-2 WT, BA.1, and BA.2 variants. Threshold of positivity has been set based on the value of the negative control (dotted line), and a nonparametric Mann-Whitney *U* test was used to evaluate the statistical significance between groups. Two-tailed *P* value significances are shown as **P* < 0.05.

drastically decreased versus the Omicron BA.1 and BA.2. In the SN2 cohort, around 20% of nAbs showed to induce phagocytosis against tested variants (Fig. 2 *B, Left*). SN3 and SP2 showed higher ability to retain ADCP against BA.1 and BA.2 even if different

trends were observed. Indeed, SN3 drove higher phagocytosis to BA.1 compared to BA.2, with NTD nAbs being the most endurable (79%), followed by S protein (66.9%) and RBD (55.2%) binders (Fig. 2 *C, Left*). As for SP2, higher phagocytosis

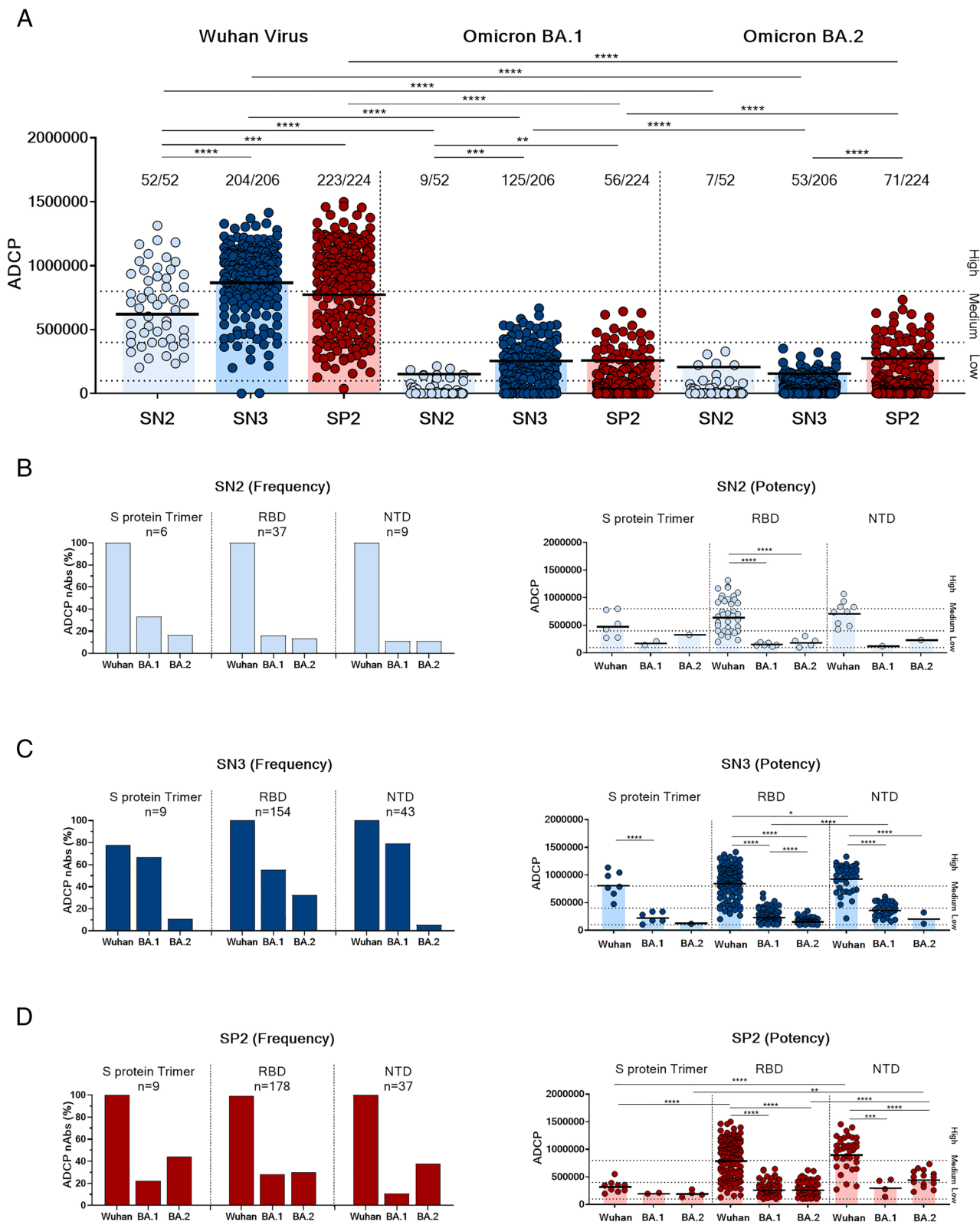


Fig. 2. ADCP driven by neutralizing monoclonal antibodies. (A) Phagocytosis induced by neutralizing antibodies isolated from SN2, SN3, and SP2 cohorts against the original SARS-CoV-2 original Wuhan virus, BA.1, and BA.2 was described. (B–D) Bar graphs show the distribution of ADCP frequency between RBD, NTD domains, and the S protein in trimeric conformation against SARS-CoV-2 original Wuhan virus, the Omicron BA.1 and BA.2 variants in the SN2 (B, Left), SN3 (C, Left), and SP2 (D, Left) cohorts. Dot plots show the ADCP potency comparison of S protein trimer, RBD, and NTD binders against SARS-CoV-2 VoCs in the SN2 (B, Right), SN3 (C, Right), and SP2 (D, Right) cohorts. A nonparametric Mann–Whitney *U* test was used to evaluate the statistical significance between groups. Two-tailed *P* value significances are shown as **P* < 0.05, ***P* < 0.01, ****P* < 0.001, and *****P* < 0.0001.

to BA.2 compared to BA.1 was observed. S protein–targeting nAbs were the most resistant to BA.2 (44.4%) followed by NTD (37.6%) and RBD (29.8%) binding antibodies (Fig. 2 D, Left).

Following, we evaluated the ADCP potency of our nAb panel (Fig. 2 B–D, Right and *SI Appendix, Table S2*). Overall, low phagocytic activity was observed in the SN2 group confirming that

a third vaccination is crucial to increase ADCP potency (Fig. 2 *B* and *C, Right*). In the SN3 cohort, NTD-targeting nAbs showed the highest ADCP against Wuhan and BA.1, while similar potency was observed for BA.2 when compared to S protein and RBD binding nAbs (Fig. 2 *C, Right*). Similarly, NTD-targeting nAbs derived from SP2 donors showed a significantly higher ADCP potency against Wuhan and BA.2 compared to S protein and RBD antibodies, while similar ADCP activity was observed against BA.1 (Fig. 2 *D, Right*).

NTD-Targeting Antibodies Are Major ADCC Drivers after a Third mRNA Vaccine Dose. As a next step, we measured the SARS-CoV-2 nAbs ability to stimulate complement deposition. Complement activation for SARS-CoV-2 antigen–antibody complex was measured using S protein expressed on the surface of target cells and detecting C3 complement deposition in presence of baby rabbit complement source. The same nAb panel described above was used to evaluate ADCC. As previously described, based on the mean fluorescent intensity value of the negative control, nAbs were classified as high (>eightfold the threshold), medium (>fourfold the threshold), or low (up to fourfold the threshold) ADCC inducers. Overall, we observed lower ADCC activity in all groups compared to ADCP (Figs. 2*A* and 3*A*). SN3 showed the highest ADCC against SARS-CoV-2 Wuhan with up to 64.6% (133/206) of nAbs activity. Differently, only 30.8% (16/52) and 48.7% (109/224) of nAbs from SN2 and SP2, respectively, showed ADCC against this virus (Fig. 3*A*). In addition, these two latter cohorts lose almost completely their ADCC activity against the Omicron variants. Only 3.8% (2/52) and 5.8% (3/52) of nAbs in the SN2 cohort showed ADCC against BA.1 and BA.2, respectively, while 7.1% (16/224) and 21.4% (48/224) of nAbs in the SP2 group induced complement deposition against these variants. As for ADCP, we evaluated a possible correlation between ADCC titers, antibody concentration, and neutralization titers. Also in this case, we observed that ADCC levels were concentration-independent (*SI Appendix*, Fig. S2*E*) and no correlation was observed between neutralization and ADCC titers for all SARS-CoV-2 variants tested (*SI Appendix*, Fig. S2 *F–H*). Following, we evaluated ADCC induced activity for S protein trimer, RBD- and NTD-targeting nAbs. NTD binding antibodies were the most active in all three cohorts against the Wuhan virus with 100% of this antibody showing activity in the SN3 cohort (Fig. 3 *B–D, Left*). Compared to ADCP, a more severe loss of ADCC was observed against BA.1 and BA.2, especially in the SN2 and SP2 cohorts, while more than 60% of NTD-binders in SN3 maintained their functionality against these variants (Fig. 3 *B–D, Left* and *SI Appendix*, Table S3). As a next step, we evaluated the ADCC potency induced by nAbs isolated from the three cohorts enrolled in this study. In line with previous results, NTD-targeting nAbs derived from the SN3 cohort triggered the highest ADCC titers against the original SARS-CoV-2 virus and the Omicron variant BA.1 (Fig. 3 *B–D, Right* and *SI Appendix*, Table S4). In the SP2 cohort, RBD and NTD Abs binders show similar potency against the Wuhan virus, but the NTD binders were the most powerful nAbs identified against the Omicron variant BA.2 (Fig. 3 *D, Right* and *SI Appendix*, Table S4).

RBD Class 3 Targeting Antibodies Induce a Strong and Variant-Resistant Fc-Mediated Response. In our previous study, RBD-targeting nAbs were classified based on their capacity to compete with the class 1/2 J08 (20), class 3 S309 (21), and class 4 CR3022 (22) antibodies (Fig. 4*A*). This information was used to understand the S protein RBD regions that mainly drive the antibody Fc-mediated response. Class 1/2, class 3, and class 4 nAbs were,

respectively, $n = 17$, 24, and 0 for SN2, $n = 98$, 30, and 3 for SN3, and $n = 114$, 48, and 7 for SP2 (17). Our results showed that almost all nAbs in the three cohorts induce ADCP against the SARS-CoV-2 Wuhan virus (Fig. 4 *B–D*), but these mAbs showed a major drop in ADCP activity against Omicron BA.1 and BA.2. Moreover, class 3 antibodies show slightly higher potency and broader protection compared to class 1/2 nAbs, especially in the SP2 cohort (Fig. 4 *B–D*). Indeed, 25.0% and 25.0% in SN2, 70.0 and 63.3% in SN3, and 54.2% and 50.0% in SP2 class 3 nAbs maintained ADCP against BA.1 and BA.2, respectively. Despite class 4 nAbs seems to induce slightly higher ADCP potency, the low number of antibodies makes difficult the comparison with the other classes of nAbs herein described. Next, we evaluated the ADCC activity of nAbs belonging to the three RBD classes of antibodies. As shown in Fig. 4 *E–G*, lower percentages of RBD-targeting nAbs induced ADCC in all three cohorts. Anyway, as described for ADCP, class 3 nAbs induced by a third booster dose or hybrid immunity showed the strongest and broadest ADCC activity against Omicron BA.1 (SN3 = 40%; SP2 = 27.1%) and BA.2 (SN3 = 70%; SP2 = 43.8%) (Fig. 4 *F* and *G*). The nAb sample size in the SN2 cohort was not sufficient to perform comparative analyses with the other groups. In addition, despite the low number, class 4 nAbs also showed ADCC levels similar to class 3 nAbs in both SN3 and SP2.

Different B Cell Germlines Are Responsible for ADCC and ADCP after Vaccination and Infection. Following the Fc functional characterization, we investigated the predominant B cell germlines and V-J gene rearrangements (IGHV;IGHJ) used by ADCP and ADCC inducing nAbs. From our panel of 482 nAbs, we retrieved 430 heavy chain sequences (SN2 = 46; SN3 = 176; and SP2 = 208) (17, 18, 23). As previously described, the most abundant germlines encoding for neutralizing antibodies were the IGHV1-69; IGHJ4-1, IGHV3-30;IGHJ6-1, IGHV3-53;IGHJ6-1, and IGHV3-66;IGHJ4-1 for SN2; IGHV1-58;IGHJ3-1, IGHV1-69;IGHJ3-1, IGHV1-69;IGHJ4-1, IGHV3-66;IGHJ4-1, and IGHV3-66;IGHJ6-1 for SN3; and IGHV1-24;IGHJ6-1, IGHV1-58;IGHJ3-1, and IGHV2-5;IGHJ4-1 for SP2 (*SI Appendix*, Fig. S3*A*) (17, 18, 23). While these were the germlines predominant for neutralization, we aimed to interrogate the B cell repertoire to understand if the same or different germlines were employed for the Fc functions evaluated in this study. The three most abundant germlines able to induce ADCP and ADCC against SARS-CoV-2 Wuhan were evaluated. Germlines showing same frequencies were included in the analyses. In the SN2 cohort, we found the IGHV3-53;IGHJ6-1 ($n = 3$; 13.0%), IGHV1-69;IGHJ3-1 ($n = 2$; 8.7%), IGHV1-69;IGHJ4-1 ($n = 2$; 8.7%), IGHV3-30;IGHJ4-1 ($n = 2$; 8.7%), and IGHV3-30;IGHJ6-1 ($n = 2$; 8.7%) (Fig. 5*A* and *SI Appendix*, Fig. S3 *B* and *C* and Table S5). These germlines accounted for 23.9% of the whole repertoire, but the number of sequences recovered was too limited for a proper evaluation of this group. In the SN3 cohort, the most abundant germlines were the IGHV1-46;IGHJ6-1 ($n = 20$; 12.7%), IGHV1-69;IGHJ4-1 ($n = 17$; 10.8%), and IGHV1-58;IGHJ3-1 ($n = 12$; 7.6%), which constituted over 27.8% of the repertoire (Fig. 5*B* and *SI Appendix*, Fig. S3 *B* and *C* and Table S5). The SP2 cohort was shown to predominantly use the IGHV1-69;IGHJ4-1 ($n = 15$; 10.0%), IGHV1-69;IGHJ3-1 ($n = 8$; 5.3%), IGHV2-5;IGHJ4-1 ($n = 8$; 5.3%), IGHV1-46;IGHJ4-1 ($n = 6$; 4.0%), and IGHV1-58;IGHJ3-1 ($n = 6$; 4.0%) germlines which represented the 20.7% of the entire repertoire (Fig. 5*C* and *SI Appendix*, Fig. S3 *B* and *C* and Table S5). Interestingly, IGHV1-69;IGHJ4-1 was the only germline publicly shared across all three cohorts. In addition, SN3 and SP2 shared also the IGHV1-58;IGHJ3-1 germline, known

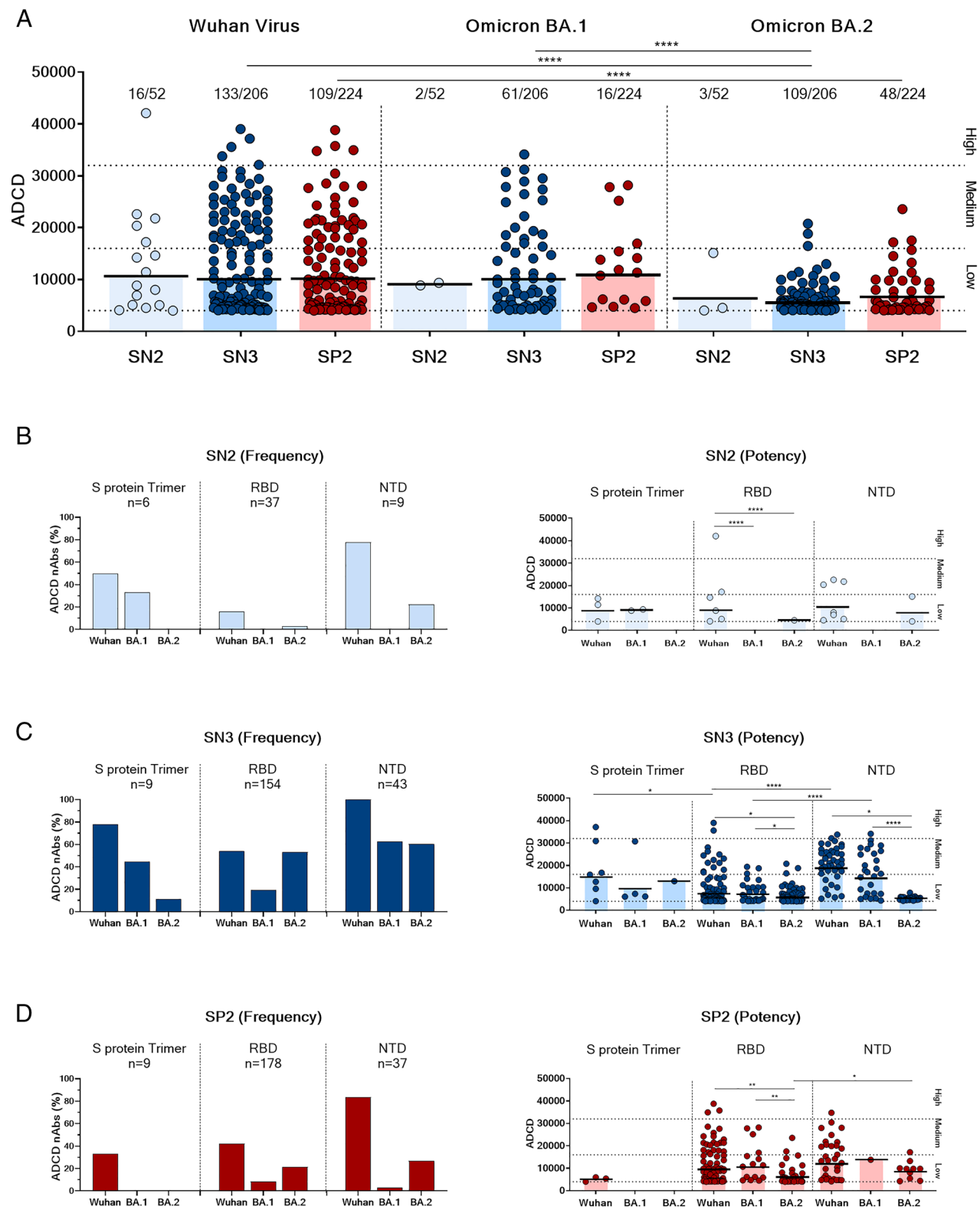


Fig. 3. ADCC response mediated by neutralizing monoclonal antibodies. (A) The graph shows antibodies dependent complement deposition against the original SARS-CoV-2 original Wuhan virus, BA.1 and BA.2 variants induced by nAbs isolated from SN2, SN3 and SP2 cohorts. (B–D) Bar graphs show the percentage of S protein, RBD and NTD nAbs binders able to induce ADCC against SARS-CoV-2 original Wuhan virus, the Omicron BA.1 and BA.2 in SN2 (B, Left), SN3 (C, Left) and SP2 (D, Left) cohort. Dot plots show the ADCC potency of S protein trimer, RBD and NTD antibodies binders against SARS-CoV-2 VoCs in SN2 (B, Right), SN3 (C, Right) and SP2 (D, Right) cohort. A nonparametric Mann–Whitney *U* test was used to evaluate the statistical significance between groups. Two-tailed *P* value significances are shown as **P* < 0.05, ***P* < 0.01, and ****P* < 0.0001.

to encode for broadly neutralizing antibodies (24). Interestingly, around 60 to 70% of predominant germlines encoding for Fc functions mediating antibodies are different from those used by

neutralizing antibodies. Indeed, only one out of three germlines (IGHV1-58;IGHJ3-1; 33.3%) in the SN3 cohort and two out of five germlines (IGHV1-58;IGHJ3-1 and IGHV2-5;IGHJ4-1;

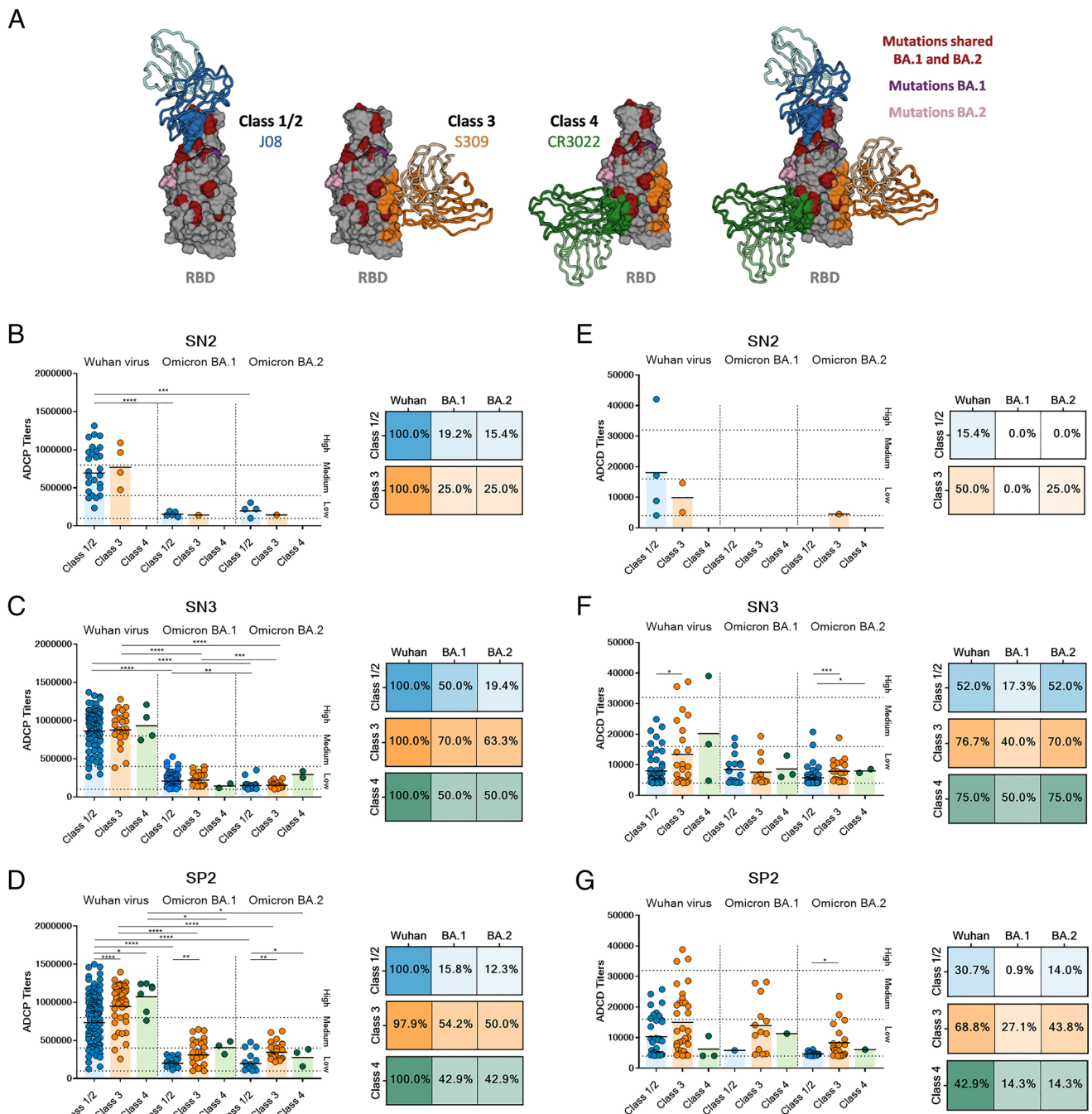


Fig. 4. ADCP and ADCC response distribution in RBD-targeting nAbs. (A) Illustration of the epitope regions recognized by class 1/2 (blue), class 3 (orange), and class 4 (dark green) RBD-binding antibodies and the distribution of Omicron mutations on SARS-CoV-2 RBD S protein. RBD residues colored in red, violet, and pink highlight mutations shared between BA.1 and BA.2 variants or specific for BA.1 and BA.2, respectively. (B–D) Dot plots show the titers of nAbs-mediated phagocytosis based on their ability to bind class 1/2, class 3, and class 4 regions on the RBD in the SN2 (B, Left), SN3 (C, Left), and SP2 (D, Left) cohorts. The heat map next to each dot plot displays the percentage of nAbs able to induce phagocytosis in the SN2 (B, Right), SN3 (C, Right), and SP2 (D, Right) cohorts. (E and F) Dot plots show the ADCC titers of class 1/2, class 3, and class 4 nAbs binders in the SN2 (E, Left), SN3 (F, Left), and SP2 (G, Left) cohorts. The heat map linked to each graph displays the percentage of nAbs able to induce complement deposition in the SN2 (E, Right), SN3 (F, Right), and SP2 (G, Right) cohorts. A nonparametric Mann–Whitney *U* test was used to evaluate the statistical significance between groups. Two-tailed *P* value significances are shown as **P* < 0.05, ***P* < 0.01, ****P* < 0.001, and *****P* < 0.0001.

40.0%) in the SP2 group responsible for ADCP and ADCC were shared with germlines predominantly used to encode for neutralizing antibodies. To better understand the differences in the Fc response from all nAbs analyzed in this study, V gene somatic hypermutations frequency was analyzed. Our data showed that SN3 nAbs had the highest level of V gene mutations followed by SP2 and SN2 (*SI Appendix*, Fig. S4 A–F). This observation could explain the higher Fc function observed in these groups compared

to the SN2 cohort. However, nAbs deriving from the same cohort, displayed similar levels of V gene mutations between RBD, NTD and S protein nAbs binders and nAbs targeting different epitope regions on the RBD (*SI Appendix*, Fig. S4 A–F). Following, we compared the ability of predominant germlines to induce neutralization, ADCP and ADCC to Wuhan, Omicron BA.1 and BA.2 (Fig. 5 D–F). The data confirmed that predominant germlines mediating Fc functions are different from those involved

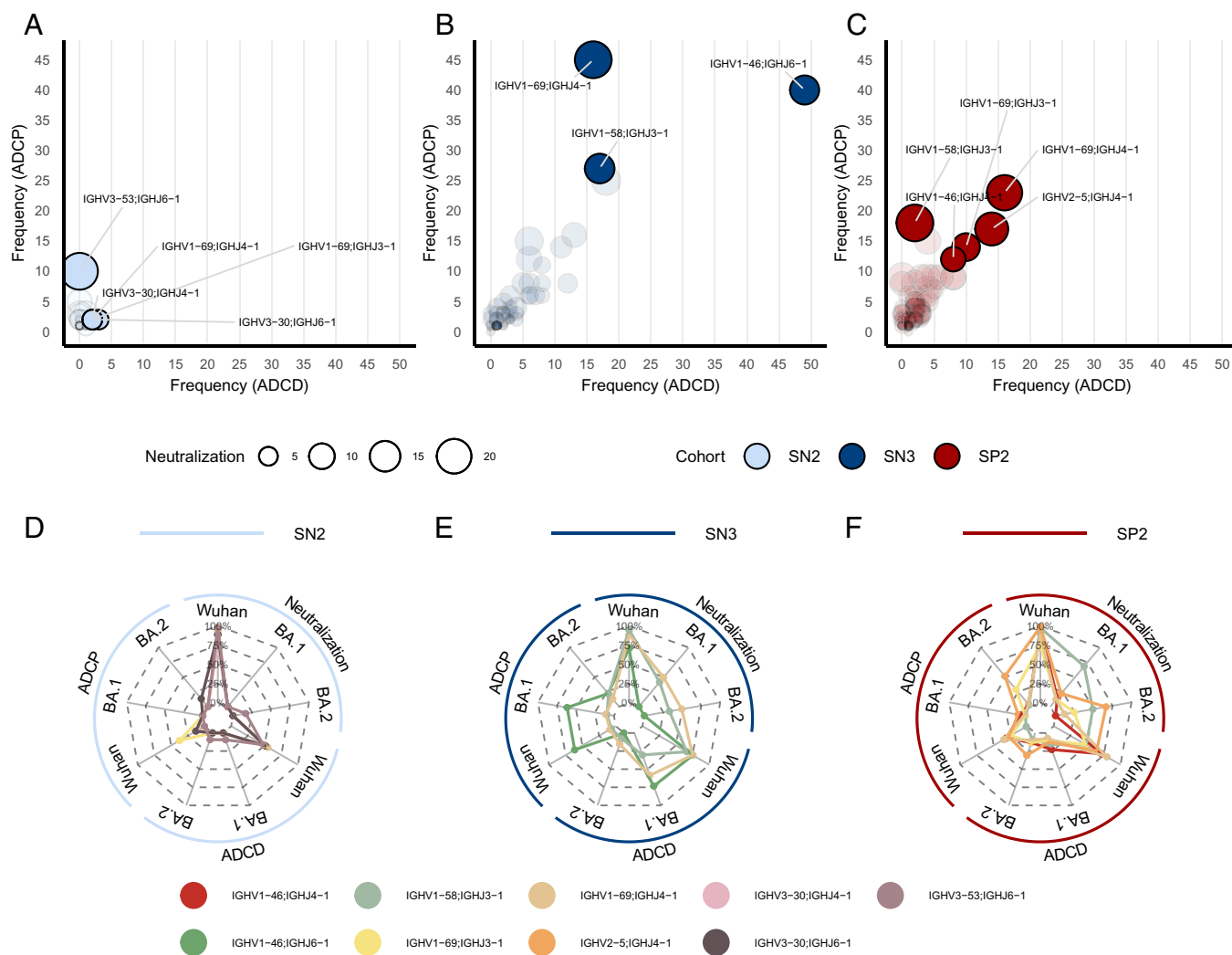


Fig. 5. IGHV;IGHJ gene rearrangements implicated in ADCP and ADCC. (A–C) Scatter plots show the B cell germline frequency for ADCP and ADCC. Light blue, dark blue, and red represent the SN2 (A), SN3 (B), and SP2 (C) cohorts. Dot sizes represent the number of antibodies derived from the same germline able to neutralize SARS-CoV-2 (D–F) Radar plots describe the neutralization, ADCP, and ADCC activities of predominant germlines identified in the SN2 (IGHV3-53;IGHJ6-1, IGHV1-69;IGHJ3-1, IGHV1-69;IGHJ4-1, IGHV3-30;IGHJ4-1, and IGHV3-30;IGHJ6-1) (D), SN3 (IGHV1-46;IGHJ6-1, IGHV1-69;IGHJ4-1, and IGHV1-58;IGHJ3-1) (E), and SP2 (IGHV1-69;IGHJ4-1, IGHV1-69;IGHJ3-1, IGHV2-5;IGHJ4-1, IGHV1-46;IGHJ4-1, and IGHV1-58;IGHJ3-1) (F). The percentages of functionality for neutralization, ADCP, and ADCC are reported within each radar plot.

in neutralization. All predominant germlines identified in the SN2 cohort showed low activities against tested variants (Fig. 5D). In the SN3 cohort, the IGHV1-46;IGHJ6-1 showed the strongest Fc-function activities against Wuhan and BA.1 variants. Interestingly, despite IGHV1-46;IGHJ6-1 antibodies showing high ADCP and ADCC against BA.1, no neutralization was observed against this variant (Fig. 5E). Finally for the SP2 group, in line with the neutralization data, the most active germline was the IGHV2-5;IGHJ4-1 which showed high ADCP and ADCC against Wuhan and the BA.2 variant (Fig. 5F).

Discussion

Given the emerging evidence of the role of Fc functions in protecting from COVID-19, we used a unique panel of 482 SARS-CoV-2-neutralizing human monoclonal antibodies to understand whether S protein domains and epitopes involved in Fc functions differ from those mediating neutralization. Antibody-mediated effector functions are influenced by both the binding of the antibody Fab region to the antigen and the affinity of the antibody Fc region to the FcR (11). To specifically

assess the domains and epitopes of the SARS-CoV-2 spike protein involved in the Fc functions, independently from the antibody isotype, we expressed all nAbs as IgG1. With our panel, we confirmed previous observations that antibodies that lose neutralization activity against variants can retain Fc functions. In addition, we made the observation that Fc functions are driven mostly by NTD- and RBD class 3–targeting nAbs while neutralization is known to be mediated mostly by RBD class 1/2 antibodies. Differences between neutralization and Fc immune responses were also confirmed by our repertoire analyses showing the use of different B cell germlines for these two functions. Interestingly, despite SN3 and SP2 show similar levels of ADCP and ADCC and to target the same epitope and domain on the S protein, they employ different germlines. This observation highlights once more how the antigenic imprinting induced by vaccination or infection shapes differently the B cell and antibody response to SARS-CoV-2. Discrepancies between the neutralization and Fc functions can also be observed by comparing the polyclonal (Fig. 1) and monoclonal responses (Figs. 2A and 3A) where the higher ADCP and ADCC activities of the SP2 polyclonal response are not reflected at the

monoclonal level. This suggests that in the polyclonal response, non-neutralizing antibodies play an important role in driving Fc functions. In conclusion, our study unravels key features of the Fc-dependent antibody effector functions and highlights the intersection between neutralization and Fc-mediated activities in subjects after vaccination or with hybrid immunity. The high-resolution picture provided in this study strongly suggests that Fc-mediating domains and epitopes should be considered to define correlates of protection, design of improved vaccines, and selection of antibodies against COVID-19.

Materials and Methods

Enrollment of COVID-19 Vaccines and Human Sample Collection. In collaboration with the Azienda Ospedaliera Universitaria Senese, Siena (IT), human samples were collected from healthy donors immunized with two or three vaccine doses and from COVID-19 convalescent who had been infected before received two vaccine doses. All subjects were immunized with the BNT162b2 mRNA vaccine, except for one subject who received the mRNA-1273 vaccine as the third dose. All the participants gave their written consent, and both sexes were included in this study. This work was approved by the Comitato Etico di Area Vasta Sud Est (CEAVSE) ethics committees (Parere 17065 in Siena) and performed according to good clinical practice and in line with the Declaration of Helsinki (European Council 2001, US Code of Federal Regulations, ICH 1997). The study was unblinded and not randomized. No statistical methods were used to predetermine the sample size.

Single-Cell RT-PCR and Ig Gene Amplification. SARS-CoV-2-neutralizing mAbs were expressed as previously described (18). Briefly, RT-PCR was performed using the cell lysate derived from the 384-cell sorting plate. Then, PCRI and nested PCR II were performed. PCR II products were purified and used to perform Gibson Assembly ligation in human Ig γ 1, Ig κ , and Ig λ expression vectors as previously described (25). Next, transcriptionally active PCR (TAP) was performed using Q5 High-Fidelity DNA Polymerase. TAP products were then purified and used for transient transfection in the Expi293F cell line following manufacturer's instructions.

ADCP Assay. Flow cytometry-based assay was used to analyze ADCP. Briefly, 200 μ g of stabilized histidine-tagged S protein was labeled using Streptavidin™XT Conjugate DY-649 (IBA Lifesciences) and coated with 1 mg of magnetic beads (Dynabeads His-Tag, Invitrogen) as previously described (18). The S protein beads were incubated with nAbs or heat-inactivated plasma diluted in complete RPMI (1:40) for 1 h at room temperature. Next, S protein beads were incubated with the monocytic THP-1 cell line overnight at 37 °C. After incubation, cells were washed with PBS (DPBS, Gibco) and fixed using fixation buffer (BioLegend) according to the manufacturer's protocol. Then, cells were washed, resuspended in 100 μ L of PBS1X, and acquired using and acquired on BD LSR II flow cytometer (Becton Dickinson). Single technical replicates were performed for each experiment. Plasma from a prepandemic healthy subject was used as negative control, and the phagocytosis score was calculated as the

percentage of THP-1 cells that engulfed fluorescent beads multiplied by the median fluorescence intensity of the population.

ADCD Assay. To investigate the antibodies' ability to induce complement deposition, Expi293F cells (Thermo Fisher, Cat#A14527) were transiently transfected with SARS-CoV-2 original S protein, BA.1, or BA.2 expression vectors (pcDNA3.1_spike_del19) using the ExpiFectamine Enhancer according to the manufacturer's protocol (Thermo Fisher). Two days later, heated-inactivated plasma diluted 1/50 in complete Expi medium (Thermo Fisher) or monoclonal antibodies were incubated with HEK-S protein cells for 30 min at 37 °C, with 5% CO₂ and 120 rpm shaker speed. Then, 50 μ L of Expi medium containing 6% of baby rabbit complement (Cedarlane) was added, and cells were incubated at 37 °C, with 5% CO₂ and 120 rpm shaker speed for 30 min. After incubation, cells were washed with PBS and stained with goat anti-rabbit polyclonal antibody against C3 (MP Biomedicals) for 1 h on ice. Cells were fixed with fixation buffer (BioLegend) for 15 min on ice. Then, cells were washed, resuspended in 100 μ L of PBS1X, and acquired using the BD LSR II flow cytometer (Becton Dickinson). Plasma isolated from a prepandemic healthy subject was used as negative control. Single technical replicates were performed for each experiment. Results were reported as median fluorescence intensity of C3 deposition on the cells.

Functional Repertoire Analyses. nAbs heavy and light chain sequences were manually curated and retrieved using the CLC sequence viewer (Qiagen). Aberrant sequences were eliminated from the dataset. Then, analyzed reads were saved in FASTA format, and Cloanalyst software was used to perform the repertoire analyses (<http://www.bu.edu/computationalimmunology/research/software/>). The figure was assembled with ggplot2 v3.3.5.

Statistical Analysis. GraphPad Prism Version 8.0.2 (GraphPad Software, Inc.) was used to perform statistical analysis. To evaluate the statistical significance between the cohorts examined in this study, a nonparametric Mann-Whitney *U* test was applied. Statistical significance was indicated as * for values ≤ 0.05 , ** for values ≤ 0.01 , and *** for values ≤ 0.001 .

Data, Materials, and Software Availability. Source data are provided with this paper. All data supporting the findings in this study are available within the article. SARS-CoV-2 antibody sequences were deposited and accessible from https://github.com/dasch-lab/SARS-CoV-2_nAb_third_dose (23). All other data are included in the manuscript and/or *SI Appendix*.

ACKNOWLEDGMENTS. This work received funding by the European Research Council advanced grant [agreement number 787552 (vAMRes)] and the Italian Ministry of Health (COVID-2020-12371817 project). In addition, this work was supported by a fundraising activity promoted by Unicoop Firenze, Coop Alleanza 3.0, Unicoop Tirreno, Coop Centro Italia, Coop Reno e Coop Amiatina.

Author affiliations: ^aMonoclonal Antibody Discovery Lab, Fondazione Toscana Life Sciences, Siena 53100, Italy; ^bData Science for Health Lab, Fondazione Toscana Life Sciences, Siena 53100, Italy; ^cDepartment of Biotechnology, Chemistry and Pharmacy, University of Siena, Siena 53100, Italy; and ^dFondazione Biotecnopolis di Siena, Siena 53100, Italy

1. World Health Organization, WHO Coronavirus (COVID-19) Dashboard. WHO. <https://covid19.who.int/>. Accessed 23 August 2023.
2. H. W. Jeong *et al.*, Enhanced antibody responses in fully vaccinated individuals against pan-SARS-CoV-2 variants following Omicron breakthrough infection. *Cell Rep. Med.* **3**, 100764 (2022).
3. P. Arora *et al.*, Omicron sublineage BQ.1.1 resistance to monoclonal antibodies. *Lancet Infect. Dis.* **23**, 22–23 (2023).
4. D. S. Khouri *et al.*, Neutralizing antibody levels are highly predictive of immune protection from symptomatic SARS-CoV-2 infection. *Nat. Med.* **27**, 1205–1211 (2021).
5. J. Pušnik *et al.*, SARS-CoV-2 humoral and cellular immunity following different combinations of vaccination and breakthrough infection. *Nat. Commun.* **14**, 572 (2023).
6. H. Zhou *et al.*, Sensitivity to vaccines, therapeutic antibodies, and viral entry inhibitors and advances to counter the SARS-CoV-2 Omicron variant. *Clin. Microbiol. Rev.* **35**, e0001422 (2022).
7. H. Gruell *et al.*, SARS-CoV-2 Omicron sublineages exhibit distinct antibody escape patterns. *Cell Host Microbe* **30**, 1231–1241.e6 (2022).
8. E. J. Nilles *et al.*, Tracking immune correlates of protection for emerging SARS-CoV-2 variants. *Lancet Infect. Dis.* **23**, 153–154 (2023).
9. A. Sigal, Milder disease with Omicron: Is it the virus or the pre-existing immunity? *Nat. Rev. Immunol.* **22**, 69–71 (2022).
10. S. R. Mackin *et al.*, Fc-γR-dependent antibody effector functions are required for vaccine-mediated protection against antigen-shifted variants of SARS-CoV-2. *Nat. Microbiol.* **8**, 569–580 (2023).
11. A. Zhang *et al.*, Beyond neutralization: Fc-dependent antibody effector functions in SARS-CoV-2 infection. *Nat. Rev. Immunol.* **23**, 381–396 (2023).
12. A. Addetia *et al.*, Therapeutic and vaccine-induced cross-reactive antibodies with effector function against emerging Omicron variants. bioRxiv [Preprint] (2023). <https://doi.org/10.1101/2023.01.17.523798> (Accessed 27 February 2023).
13. S. Jegaskanda, H. A. Vanderven, A. K. Wheatley, S. J. Kent, Fc or not Fc; that is the question: Antibody Fc-receptor interactions are key to universal influenza vaccine design. *Hum. Vaccin. Immunother.* **13**, 1288–1296 (2017).
14. D. J. DiLillo, P. Palese, P. C. Wilson, J. V. Ravetch, Broadly neutralizing anti-influenza antibodies require Fc receptor engagement for in vivo protection. *J. Clin. Invest.* **126**, 605–610 (2016).
15. B. M. Gunn *et al.*, A role for Fc function in therapeutic monoclonal antibody-mediated protection against Ebola virus. *Cell Host Microbe* **24**, 221–233.e5 (2018).

16. M. Troisi *et al.*, A new dawn for monoclonal antibodies against antimicrobial resistant bacteria. *Front. Microbiol.* **13**, 1080059 (2022).
17. E. Andreano *et al.*, mRNA vaccines and hybrid immunity use different B cell germlines against Omicron BA.4 and BA.5. *Nat. Commun.* **14**, 1734 (2023).
18. E. Andreano *et al.*, Hybrid immunity improves B cells and antibodies against SARS-CoV-2 variants. *Nature* **600**, 530–535 (2021).
19. E. Andreano *et al.*, B cell analyses after SARS-CoV-2 mRNA third vaccination reveals a hybrid immunity like antibody response. *Nat. Commun.* **14**, 53 (2023).
20. J. L. Torres *et al.*, Structural insights of a highly potent pan-neutralizing SARS-CoV-2 human monoclonal antibody. *Proc. Natl. Acad. Sci. U.S.A.* **119**, e2120976119 (2022).
21. D. Pinto *et al.*, Cross-neutralization of SARS-CoV-2 by a human monoclonal SARS-CoV antibody. *Nature* **583**, 290–295 (2020).
22. M. Yuan *et al.*, A highly conserved cryptic epitope in the receptor binding domains of SARS-CoV-2 and SARS-CoV. *Science* **368**, 630–633 (2020).
23. G. Maccari, Data for the manuscript "COVID-19 mRNA booster dose induces hybrid immunity-like antibody response". GitHub. https://github.com/dasch-lab/SARS-CoV-2_nAb_third_dose. Deposited 12 December 2022.
24. T. Zhou *et al.*, Structural basis for potent antibody neutralization of SARS-CoV-2 variants including B.1.1.529. *Science* **376**, eabn8897 (2022).
25. E. Andreano *et al.*, Extremely potent human monoclonal antibodies from COVID-19 convalescent patients. *Cell* **184**, 1821–1835.e16 (2021).